Title: Exploring uncertainty of Amazon dieback in a perturbed parameter Earth system ensemble

Running Head: Exploring Amazon dieback uncertainty

Authors: Chris A. Boulton[1]*, Ben B. B. Booth[2], Peter Good[2]

Affiliations: [1]Earth System Science, College of Life and Environmental Sciences, University of Exeter, Exeter EX4 4QE, UK

[2]Met Office Hadley Centre, FitzRoy Road, Exeter, EX1 3PB, UK

Correspondence: email:c.a.boulton@exeter.ac.uk

Keywords: 'Amazon rainforest', 'Physics-perturbed ensemble', 'HadCM3C', 'Climate uncertainty', 'Committed response'

Article Type: Primary Research Article

Abstract

The future of the Amazon rainforest is unknown due to uncertainties in projected climate change and the response of the forest to this change (forest resiliency). Here we explore the effect of some uncertainties in climate and land surface processes on the future of the forest, using a perturbed physics ensemble of HadCM3C. This is the first time Amazon forest changes are presented using an ensemble exploring both land vegetation processes and physical climate feedbacks in a fully coupled modelling framework. Under three different emissions scenarios, we measure the change in the forest coverage by the end of the 21st century (the transient response), and make a novel adaptation to a previously used method known as 'dry-season resilience', to predict the long term committed response of the forest, should the state of the climate remain constant past 2100. Our analysis of this ensemble suggests that there will be a high chance of greater forest loss on longer timescales than is realised by 2100, especially for mid-range and low emissions scenarios. In both the transient and predicted committed responses, there is an increasing uncertainty in the outcome of the forest as the strength of the emissions scenarios increase. It is important to note however that very few of the simulations produce future forest loss of the magnitude previously shown under the standard model configuration. We find that low optimum temperatures for photosynthesis and a high minimum leaf area index needed for the forest to compete for space appear to be precursors for dieback. We then decompose the uncertainty into that associated with future climate change and that associated with forest resiliency, finding that it is important to reduce the uncertainty in both of these if we are to better determine the Amazon's outcome.

Introduction

There is currently a large focus on the future stability of the Amazon rainforest. This is due to its roles as an important carbon store and current sink in the climate system (Malhi *et al.*, 2008). Significant loss, or dieback, of the rainforest could result in this carbon sink becoming a source, releasing stored carbon which would contribute to atmospheric CO_2 and so in turn climate change. Aside from this, the Amazon rainforest is important for other reasons such as sustaining large biodiversity (Dirzo & Raven, 2003).

General circulation models (GCMs) give some insight into the future responses of the rainforest, projecting climate change forced by emissions scenarios, and the forest's response to this. Uncertainties in the future forest response due to different components of the Earth system represent an ongoing challenge, with work exploring the impact of land uncertainties to an atmospheric climate change (Cramer *et al.*, 2004, Galbraith *et al.*, 2010, Scholze *et al.*, 2006, Sitch *et al.*, 2008), uncertainty in atmospheric drivers on a surface vegetation model (Rammig *et al.*, 2010, Salazar *et al.*, 2007) or on bioclimatic regions (Malhi *et al.*, 2009) all readily found in current literature. Poulter *et al.*, (2010) and Huntingford *et al.*, (2013) both attempt to synthesise uncertainties from both land and atmosphere.

Amazon forest dieback was first simulated in an offline vegetation model when forced by climate change occurring in HadCM3 (White *et al.*, 1999). Since then, it has also been found in some coupled GCMs such as HadCM3LC (Cox *et al.*, 2000). Results from the standard version of the Hadley Centre's model show much larger dieback compared to simulations from most other Dynamic Global Vegetation Models (DVGMs) (Galbraith *et al.*, 2010, Huntingford *et al.*, 2013). This is due to strong regional drying and warming that overwhelm the rising atmospheric CO_2 that contributes to increased photosynthesis (via the CO_2 fertilisation effect) and thus productivity of the Amazon rainforest (Cox *et al.*, 2004, Good *et*

68 *al.*, 2011, Good *et al.*, 2013, Huntingford *et al.*, 2013, Malhi *et al.*, 2009). This does not
69 necessarily mean the response in the Hadley Centre's model is implausible; Shiogama *et al.*,
70 (2011) used observational constraints to suggest that the CMIP3 ensemble mean
71 underestimates the most likely level of drying over the central/eastern Amazon. Nevertheless,
72 the differences between current projections suggest that the forest's future is uncertain.

73 There has been much research into the varied responses of the forest under different GCMs
74 and Dynamic Global Vegetation Models (DGVMs). For example Sitch *et al.*, (2008) test a
75 variety of DGVMs under different emissions scenarios whilst using the same GCM. More
76 recently, Huntingford *et al.*, (2013) test the effect of climate change patterns from 22 GCMs
77 which explore changes in land vegetation processes (Booth *et al.*, 2012), whilst using a single
78 DGVM (TRIFFID) (Cox, 2001). They then analyse biomass changes of the forest in the
79 ensemble used here, along with Sitch *et al.*'s, (2008) changes due to DVGM differences to
80 determine there is a larger uncertainty associated with future emissions scenarios than climate
81 model uncertainty. These works explore uncertainty in the future of the Amazon rainforest by
82 focusing on specific modelled components (e.g. forest resiliency and climate change
83 respectively). Poulter *et al.*, (2010) perturb parameter values within the LPJmL DGVM and
84 combine this with an ensemble of 8 GCMs to determine which parameters are most important
85 in reducing uncertainty of future Amazon rainforest response. Galbraith *et al.*, (2010) use
86 factorial simulations to determine the effect certain factors, such as temperature or
87 precipitation changes, have on vegetation carbon in the Amazon region for three DVGMs.

88 Here we explore uncertainty in Amazon forest projections using output from a 57-member
89 perturbed-physics ensemble of HadCM3C (Booth *et al.*, 2013), a GCM whose Amazon
90 dieback in its standard configuration is at the upper end of current projections. Our
91 uncertainties in future climate change and forest resiliency are represented by the processes
92 that are perturbed in the ensemble, allowing the opportunity to determine how sensitive future

Amazon forest change is to these. This ensemble explores both land vegetation processes and physical climate feedbacks and represents the first time future Amazon rainforest changes have been analysed with this uncertainty. Furthermore, this is all carried out within a fully-coupled framework meaning there is no mismatch between atmospheric drivers and changes in surface conditions. This aspect of our framework is unique. This also allows the vegetation to feedback on the atmosphere, both locally and globally. We run our ensemble under 3 different emissions scenarios.

The modelled vegetation in the Amazon rainforest (as well as vegetation elsewhere) exhibits inertia, meaning there is a delay in the response of the forest to the climate change that has occurred. The eventual response based on the climate change that has happened up to a certain time, known as the 'committed response', can take decades to be realised (Jones *et al.*, 2009). This response may be calculated using 'equilibrium vegetation' simulations where the climate is held at a constant level, allowing the vegetation to settle to equilibrium (Cox, 2001, Jones *et al.*, 2009). In a transient scenario (where radiative forcing was steadily increasing), Jones *et al.*, (2009) found that Amazon dieback lagged the committed forest change by around 50 years. Because of this, the transient forest response could be considered a lower bound to the potential long term forest loss that would occur in the model without reversing climate change. Understanding this committed response is important in determining the longer term outcome of the forest to emissions over the 21st century as, for example, the area of sustainable forest coverage may be significantly reduced well before transient loss is observed. Huntingford *et al.*, (2013) calculate the committed response for the 22 models they test and find that rainforests that are growing in the transient experiment continue to grow slightly whereas rainforests which have 'peaked' and are on a decline show more dieback in their eventual committed response.

The primary controls on the large-scale distribution of committed vegetation under present-day through future conditions are rainfall, temperature and atmospheric CO_2 concentration. Good *et al.*, (2011, 2013) showed that for Hadley Centre models, while considering tropical (20°N-20°S) land, combinations of dry-season length, the number of months a year that precipitation falls below a certain threshold or produce a water deficit, and temperature promote sustainable forest. There is no forest found in areas which are too warm or dry (i.e. have a long dry-season length). Dry-season length is closely related to Malhi *et al.*'s, (2009) maximum cumulative water deficit (MCWD) calculation, which combines information on the dry-season rainfall level as well as the dry-season length. In these Hadley Centre model simulations at least, the boundary between sustainable forest and no forest is fairly distinct.

In turn, Amazon rainfall anomalies have been linked to sea surface temperature indices in both the tropical Pacific (Cox *et al.*, 2004, Harris *et al.*, 2008) and Atlantic (Cox *et al.*, 2008, Good *et al.*, 2008, Harris *et al.*, 2008). Both of these indices are observable in the real world. Furthermore, increased rainfall comes from air that has passed over extensive vegetation suggesting that precipitation changes are also linked to deforestation (Spracklen *et al.*, 2012). Using observed precipitation values in tropical rainforest areas, potential analysis (Livina *et al.*, 2010) has been used to determine how vulnerable certain areas of the forest are (Hirota *et al.*, 2011) which is related to how far away they are from the boundary of not having enough precipitation to sustain themselves.

Dieback of the Amazon rainforest has been considered a tipping point in the Earth system (Lenton *et al.*, 2008) and generic early warning signals based on time-series analysis of variance, autocorrelation and skewness (Lenton, 2011) have also been tested on output of the ensemble of HadCM3C used here (Boulton *et al.*, 2013). However due to the slower dynamics of the system (the committed response of the forest) compared to fast, anthropogenic forcing, the generic early warning signals do not show much promise and

indicators based on the physical processes of the Amazon rainforest appear to be the more of a prospect. Aside from determining uncertainty of the future of the rainforest, we also hope the methods described in this paper could progress future work towards a more 'system-specific' indicator of approaching a tipping point rather than the more generic early warning signals which have been shown to fail in this instance.

As well as analysing the transient response of the Amazon rainforest by 2100 under 3 emissions scenarios for each ensemble member, we also predict the long term committed change of the forest, which would not be realised for many decades beyond 2100. To do this, we present a novel use of the dry-season resilience method described earlier (Good *et al.*, 2011). While Galbraith *et al.*'s, (2010) analysis suggests that TRIFFID (Cox, 2001), the DGVM used in HadCM3C and HadCM3LC, is insensitive to a drying climate in regards to changes in vegetation carbon compared to an increasing temperature, Good *et al.*, (2011) suggest that both are equally important.

Materials and methods

HadCM3C-ESE

Our data is obtained from the HadCM3C Earth System Ensemble (HadCM3C-ESE) (Lambert *et al.*, 2013), using the TRIFFID DGVM (Cox, 2001) to determine the vegetation distribution. This model configuration differs from the HadCM3LC build used in many earlier Amazon dieback studies in that it runs with a higher ocean resolution and couples in a fully interactive (both direct and indirect) sulphate aerosol scheme (Booth *et al.*, 2012). However, importantly the formulation of the DGVM remains the same between the two. There are 57 model configurations within the ensemble, each containing a different combination of perturbed parameters. The parameters are perturbed within boundaries

suggested either by observational ranges or expert elicitation and grouped according to their role within the Earth system, whether they are part of the carbon cycle (n=8 parameters) (Booth *et al.*, 2012), atmosphere (n=32) (Collins *et al.*, 2011), sulphur cycle (n=8) (Lambert *et al.*, 2013) or ocean (n=15) (Collins *et al.*, 2007). A Latin hypercube sampling method was used to sample a range of combinations of carbon cycle and atmosphere parameters (Lambert *et al.*, 2013). There were originally 68 members, however 11 were removed from the ensemble for failing to simulate reasonable top of the atmosphere (TOA) radiative fluxes during the spin up (outside the bounds suggested by Collins *et al.*, (2011)). Ensemble members that failed to simulate the presence of Amazon or boreal forests were also removed (Lambert *et al.*, 2013). The ensemble is driven by emissions profiles expected to give the trajectories explained below (much like Meinshausen *et al.*, (2008)). This means that atmospheric greenhouse gas concentrations are prognostic values and vary due to different emergent model sensitivities resulting from the underlying perturbed parameters sampled in these experiments, even under the same emissions scenario. If the direct forcings or concentrations were applied to the ensemble members, it would prevent the opportunity to explore global feedbacks in the carbon cycle and thus by using emissions profiles, more uncertainty is explored.

Previous work comparing the Amazon region observations to those of members of a multi-model ensemble suggests that models are generally too dry and that accounting for this produces less dieback (Malhi *et al.*, 2009). To determine how well our ensemble simulates real world climate, we compare the Amazon rainforest temperature and dry-season length of each member to observations from CRUTEM3 (Brohan *et al.*, 2006) and GPCC (Schneider *et al.*, 2014). By comparing the average Amazon climate state in the temperature-dry-season length plane to that of the real-world (Fig. 1a), we find that the observations lie within a reasonable range of our simulations as the ensemble members have Amazon region

191 temperature and dry-season length ranges that encompass the observations (Fig. 1b,c).
192 HadCM3C-ESE has been run under 3 scenarios, a mitigation scenario RCP 2.6 (van Vuuren
193 *et al.*, 2006, van Vuuren *et al.*, 2007) , a balanced scenario, SRES A1B (Nakicenovic *et al.*,
194 2000) and a business as usual scenario, RCP 8.5 (Riahi *et al.*, 2007), as detailed by Booth *et*
195 *al.*, (2013). By using this ensemble and these scenarios, we are able to explore the uncertainty
196 in the future of the forest associated with climate and parameter (which in turn determine
197 forest resiliency) unknowns. General comparisons between each scenario's model outputs,
198 such as global mean temperature, have been shown elsewhere (Booth *et al.*, 2013). Each of
199 the scenarios share a common historical driving dataset from 1860-1950 based on SRES data,
200 after which parallel SRES and RCP historical simulations were run. These form the basis
201 from which A1B (from 1990) and the 2 RCPs (from 2005) were extended from. Further
202 details about the experimental setup are described by Booth *et al.*, (2013).

203 HadCM3C-ESE was originally created to explore the spread of results capable under
204 HadCM3C dynamics, rather than to determine the effects of individual parameters on
205 changes in vegetation. For this, single parameters would have to be perturbed whilst keeping
206 others constant. However we explored the relationship between the transient responses and
207 land surface parameters perturbed in the ensemble, noting that the full effect of each
208 parameter is difficult to determine. A selection of the parameters concerned with the carbon
209 cycle (Booth *et al.*, 2012) are shown in Table 1 with a short description and the ranges they
210 are sampled from. Parameters from the other groups (detailed previously) are less influential
211 on forest resiliency and are not included in Table 1. Note that some perturbed parameter
212 values are assigned to each plant functional type (PFT) in the ensemble, however Table 1
213 only shows the ranges for the broadleaf fraction PFT (which we use to measure forest cover).
214 Ranges of the other PFTs have been detailed by Booth *et al.*, (2012).

215

Estimating the committed forest response: modified dry-season resilience method

The basis of our analysis is to determine climate conditions that sustain forest and to explore the long term committed response of the forest (Jones *et al.*, 2009), to projected climate changes. Forest is considered sustainable if it exists at equilibrium (once transient dynamics have been resolved) for a given climate. Our method is based on that of Good *et al.*, (2011).

The method of Good *et al.* as tested on the standard version of the lower resolution HadCM3CL (Good *et al.*, 2011) and HadGEM2-ES (Good *et al.*, 2013), aims to quantify climate drivers that affect sustainable forest. It does this by using annual mean temperature and annual dry-season length (DSL, the number of months in a year that monthly precipitation is below 100mm) from land grid points in the tropics (20°S-20°N), as well as global atmospheric CO_2 concentration as climate drivers that affect sustainability.

There is a large range of dry-season lengths found in the ensemble (Fig. 2), both when using the mean forest climate from each ensemble member (Fig. 2a) and the individual grid points from all ensemble members (Fig. 2b). Furthermore these DSL values are highly correlated with their corresponding MCWD values (Malhi *et al.*, 2009) (r=0.898 for the 1860-1950 state and r=0.963 for the 2080-2100 state when using the ensemble forest mean values, Fig. 2a), suggesting that using the number of months the forest is under water stress, rather than the amount it is stressed by, in our calculations is a simple replacement.

To determine climate conditions that are suitable for sustainable forest, equilibrium broadleaf tree fraction (BL) is plotted in the temperature-dry-season length plane for a given model configuration (see Fig. 3a for an example using our method). The points are coloured depending on whether there is forest (green, BL > 0.4), an intermediate amount of forest (blue, 0.05 < BL < 0.4) or no forest (red, BL < 0.05). We have also circled points contained within a region we define as the Amazon rainforest (40°-70°W, 15°S-5°N) as the climate

changes in these points are what we are most interested in. Fig. 3a shows two distinct regions: one where climate promotes sustainable forest growth and a region which does not contain forest. The boundary between the two regions is approximately linear, so is quantified with a linear fit of the form shown in Eqn. (1).

$$DSR = DSL + \alpha T + \gamma CO_2 + c \quad (1)$$

DSR (in units of months) is dry-season resilience, a measure of the resiliency of a grid point to changes in climate. Visually, *DSR* refers to the distance away from the boundary between forest and no forest a grid point is with *DSR*=0 on the boundary itself, suggesting points on the boundary have no resilience to climate change (an increase in temperature or dry-season length; Fig. 3a). *DSL* and *T* refer to the dry-season length and temperature of a given grid point respectively whereas CO_2 is the global mean value of atmospheric CO_2. The coefficients α and γ, the temperature sensitivity and CO_2 fertilisation coefficient respectively, are to be determined along with the constant *c*. With this formulation, we are able to make statements such as 'if DSL were to increase by a month, then temperature would have to decrease by α for the grid point to have the same resilience'. The parameters α, γ and *c* in Eqn. (1) are dependent on the parameters perturbed within the ensemble and as such there is uncertainty associated with them, which we will later decompose.

Good *et al.* originally estimated these parameters on equilibrium runs, where the vegetation has settled to equilibrium under a constant climate. The parameters are calculated through the use of an algorithm that minimises the number of grid points that are on the wrong side of the boundary.

To fit the parameters for this ensemble, we adapt the above method. Equilibrium vegetation simulations were not available, due to computational expense associated with the large ensemble size (this would involve carrying out 57 additional full GCM experiments for each

of the 3 future scenarios explored in this study). Using the fact that the 3 scenarios used the same historical simulation from 1860-1950, as well the climate staying relatively stable during this time, we treat this as a 'quasi-equilibrium' early industrial state to begin our analysis from. For each land grid point in the tropics (20°N-20°S) within each configuration, we calculate the average temperature, dry-season length and the average broadleaf (BL) fraction over these 90 years. We also extract the 1860-1950 mean global CO_2 (ppm) value for each ensemble member.

Our modification of the original DSR method is to use a logistic regression fit to estimate the parameters in equation 1, focusing around the transition from forest to no forest by using only grid points with temperature, $T > 10$°C and $4 < DSL < 10$ and fitting the line to where BL=0.025, the midpoint of the blue, intermediate values of forest in Fig. 3a. This standardised method of computing α and c is much more efficient than using the original method to determine them for all 57 ensemble members.

An important caveat here is that by using equilibrium runs in their analysis, Good *et al.*, (2011) were able to infer the value of γ, the CO_2 fertilisation coefficient (equal to 0.0043) from the lower resolution, standard configuration, HadCM3LC by running a parallel model with double the atmospheric CO_2 concentration. We use their value in our analysis as we do not have the simulations required to estimate this fertilisation coefficient for each individual configuration. These extra runs would have allowed us to have two values for atmospheric CO_2 from which we would be able to infer the fertilisation coefficient through the use of our logistic regression fit each time. Instead we are making the simplification that the CO_2 fertilisation effect does not vary between simulations, although it is important to note that the true value of γ in each instance is dependent on the parameters perturbed for each configuration. We note that only the fertilisation coefficient γ is kept constant across all

288 configurations and that the fertilisation effect itself will differ depending on the global
289 atmospheric CO_2 concentration.

290 We have however run 10 ensemble members to equilibrium by holding climate forcings
291 constant at their 2100 level, whilst allowing climate and the forest to respond since they lag
292 the forcings (Fig. 4). This subset was chosen as it represents a range of parameter
293 configurations, namely a spread in T_{OPT} (Table 1). We use these runs to test the validity of the
294 linear regression described above, finding that temperature becomes a limiting factor in forest
295 sustainability. However we note that for the range of temperature observed up to 2100, the
296 linear regression appears to be valid.

297 After determining the temperature sensitivity α and constant c for each configuration, Eqn.
298 (1) allows a prediction of whether broadleaf forest is sustainable or not at each location for
299 each year based on its dry-season resilience (DSR) value (Eqn. (1)), given the prevailing
300 climate. First we calculate the number of points in the Amazon region that are below the
301 DSR=0 line in our quasi-equilibrium (1860-1950) state in each of our configurations. We
302 then calculate the number of points that are below the line using the 2080-2100 average from
303 each simulation. In effect, we are using DSR as a method of extrapolation to estimate the
304 state of the committed Amazon rainforest without running a corresponding equilibrium run
305 for each ensemble member. A prediction on the post-2100 equilibrium state of a grid point is
306 based on the equilibrium state of a grid point with similar climate in the quasi-equilibrium
307 state. Due to the CO_2 fertilisation effect, increases in atmospheric CO_2 cause the boundary
308 line (DSR=0) to move upwards. Consequently moderately increased temperatures and dry-
309 season lengths can sustain forest under the higher atmospheric CO_2 values. An example of
310 these changes over the 21st century is shown in Fig. 3b. We use the 20 year averages to
311 eliminate year-to-year variability. The difference between the 1860-1950 and 2080-2100

values gives us our prediction of committed change. The combined result of the configurations from each emissions scenario gives us a measure of uncertainty of the future behaviour of the Amazon rainforest and its committed response to 21st century climate change.

Results

Transient responses

Time series of the transient responses of the Amazon rainforest up to 2100 in HadCM3C-ESE are shown in Fig. 5a. These responses are calculated as the proportional change in the number of Amazon region (40°-70°W, 15°S-5°N) grid points that exhibit forest (i.e. $BL > 0.4$) between 2000 and 2100.

Unlike the standard configuration of HadCM3LC (Cox *et al.*, 2000), the majority of the simulations show little change by the end of the 21st century (Fig. 5a). However there are simulations which show dieback at similar levels to that of the forest in the standard model and even greater. This suggests that the land surface configuration used in previously published Hadley Centre studies lies in the upper end of the range of projected dieback given the parametric uncertainties, and most model configurations suggest smaller magnitude changes. However, it is still within the envelope of uncertainty provided by this ensemble.

When partitioning the transient responses by scenario (Fig. 5b), there is an increasing uncertainty in the forest state at 2100 with increasing strength of emission scenarios. Under the RCP 2.6 mitigation scenario, we see that the mean transient response is no change to the forest cover with a few simulations showing dieback, giving a negatively skewed distribution. For A1B simulations, while the mean response still suggests no change, it is clear there is

more of a tendency for forest loss to be exhibited than occurs under mitigation. Under RCP 8.5, the mean response decreases slightly to a loss of around 5%. The uncertainty however is a lot greater. As well as having more members which show loss and dieback, there are also more simulations that have forest growth than the other two scenarios.

The simulation with the largest dieback that occurs in RCP 2.6 shows signs of forest loss by 2040 and does so in all three scenarios. For the forest to dieback so soon in the century suggests that in some cases, the configuration of perturbed parameters can cause forests that are already very near the threshold of dieback under present day conditions rather than emissions causing this.

While linking regional climate changes to specific physical parameters is not possible in this ensemble, it is more feasible to identify land-surface parameters affecting forest resilience. When determining if any of the perturbed land-surface parameters were linked to forest loss, we found the strongest relationships (Fig. 6) were found between forest change and T_{OPT} (the optimum temperature for photosynthesis) and *minLAI* (a competition parameter specifying the minimum leaf area index a plant functional type needs before it begins to compete for space). If temperatures get much higher than T_{OPT} then there will be a decline in photosynthesis. We are looking at the spread of the forest in our analysis and thus if *minLAI* is too high then the forest will not compete for space and so will dieback and the space will be taken over by other plant functional types. Using results from RCP 8.5, which have the largest spread of transient responses, analysis on the combination of T_{OPT} and *minLAI* on forest change (Fig. 6) shows low values of T_{OPT} and high *minLAI* for broadleaf preconditions dieback (consistent with the physiological roles played by these parameters). Members with a T_{OPT} of greater than 32°C show no extreme dieback (although less extreme loss is still observed, Fig. 6a). Likewise, members with a *minLAI* less than 2.5 show no extreme dieback (Fig. 6b), whereas members with stronger dieback have a T_{OPT} less than 32°C and a *minLAI*

360 greater than 2.5 (Fig. 6a,b). However other factors such as changes in climate that would
361 stress the forest, as well as the values of other parameters not explored, will determine if
362 dieback does occur. Although there are less members which show dieback under the A1B
363 scenario, the boundaries for T_{OPT} and *minLAI* seem consistent (Fig. 6c,d). This further
364 strengthens the argument that although other factors such as climate change, which is not as
365 strong in the A1B scenarios, drive dieback, low T_{OPT} combined with high *minLAI* is
366 potentially a precondition. The values of *minLAI* and T_{OPT} in the standard configuration (Cox
367 *et al.*, 2000) (3 and 32°C respectively) are near the thresholds that precondition dieback (Fig.
368 6). This could explain, at least partially, why dieback is observed in the standard model, but
369 not in the majority of the ensemble.

370

371 Committed response predictions

372 To compare the transient responses (those in Fig. 5) to our predictions of the committed
373 responses (calculated using our modified DSR method), we present the results in the form of
374 cumulative density functions (CDFs, Fig. 7).

375 In all three scenarios, our prediction of committed change suggests there is more uncertainty
376 in the eventual outcome of the forest with a higher chance of further forest loss than is
377 realised by 2100 (the transient response). For example under RCP 2.6, the mitigation
378 scenario, there is fairly robust response of 'No change' (forest remains within 5% of its
379 original size) by 2100 (Fig. 7a). However over 40% of models predict a committed 'Loss'
380 (>5% decrease) or 'Dieback' (>25% decrease) (Fig. 7d). Similar results are observed for the
381 other two scenarios (A1B; Fig 7b,e, and RCP 8.5; Fig. 7c,f). However the least amount of
382 models predicting large committed forest loss are found under the mitigation scenario.

383 In both the transient and predicted committed responses of the forest, stronger emissions
384 scenarios (increased CO_2 emissions for example), lead to an increasing uncertainty in the
385 resulting forest change with more of a tendency towards forest loss. However like the
386 transient response, there are also more RCP 8.5 ensemble members where forest 'Growth'
387 (>5% increase) is predicted as a committed response when compared to the other scenarios
388 the other scenarios. This suggests more spread and thus more uncertainty in future outcome
389 of the forest under stronger emissions scenarios. This uncertainty is also noted by the gradient
390 of the CDFs as steeper gradients suggest less uncertainty.

391

392 Decomposing uncertainty

393 To begin to determine causes in the spread of committed responses predicted, we decompose
394 the uncertainty into that associated with climate change, and that associated with forest
395 resiliency (the coefficient α, the temperature sensitivity, and c in Eqn. (1), previously
396 calculated individually for each of the 57 configurations). This analysis is carried out on the
397 RCP 8.5 scenario runs as out of the three scenarios, these had the largest predicted committed
398 spread (Fig. 7).

399 Decomposing the uncertainty is achieved by keeping one set of parameters (either climate
400 change or forest resiliency parameters), constant whilst allowing the other to vary and
401 repeating the analysis used to predict the committed response. The uncertainty associated
402 with the climate change component is explored by fixing the values of temperature sensitivity
403 α and constant c in Eqn. (1) for each model to the ensemble mean values. This holds the
404 forest resiliency constant. Fig. 8a shows the average forest resiliency (red DSR=0 line). As
405 the climate is still allowed to change, movement of the grid points over the 21st century as
406 well as movement of the DSR=0 due to increasing atmospheric CO_2 will occur. Similarly,

407 uncertainty associated with forest resiliency is explored by fixing the climate at each location
408 in each model to the ensemble mean (Fig. 8b shows the average climate change for an
409 example grid point – see red line).

410 Compared to our overall prediction uncertainty (Fig. 9a – solid line), we find that our
411 uncertainty in climate change, under the RCP 8.5 emissions scenario is similar (Fig. 9a –
412 dashed line). This suggests the largest proportion of overall uncertainty is explained by
413 uncertainties in the climate, compared to uncertainty in forest resiliency (Fig. 9a – dotted
414 line), which has less of a spread of results (but still shows some uncertainty).

415 We further constrain our uncertainty in climate change by using real world observations of
416 temperature from the CRUTEM3 dataset (Brohan *et al.*, 2006) and dry-season length from
417 the GPCC precipitation dataset (Schneider *et al.*, 2014) to use as starting positions for each
418 grid point. Due to observational constraints, rather than using 1860-1950 as our quasi-
419 equilibrium state, we instead use a 1950-1980 average. Using real world observations
420 eliminates the uncertainty associated with the starting position of each grid point in the
421 temperature-DSL plane. Then the equivalent of the 2080-2100 mean state of a grid point is
422 achieved by adding the climate change in the model between 1860-1950 and 2080-2100 onto
423 the real world observations (Fig. 8c). Using these real world observations, we decompose the
424 uncertainty again as we have described above. By doing this, we are able to compare how our
425 uncertainty in forest resiliency compares to our uncertainty in future climate change,
426 eliminating uncertainty in what we already know about recent past climate.

427 When initialising our analysis using the real world observations as the starting climate (Fig.
428 9b – solid line) we again find that our uncertainties associated with climate change are still
429 large (Fig. 9b – dashed line). Indeed, fixing the starting climate has a rather small effect on
430 the range of projections in this ensemble. However proportionally there is more spread in

forest outcome while exploring the uncertainty in forest resilience (Fig. 9b – dotted line) than previously (Fig. 9a). This suggests that forest resiliency is important to understand as well as future climate change.

Discussion

HadCM3C-ESE responses

We explore the future forest response to uncertainties in both land vegetation processes and physical climate feedbacks. These suggest a range of transient forest responses consistent with uncertainties in current climate model parameters. This shows that the result of ~60% dieback from the standard HadCM3LC model (Cox *et al.*, 2000) is not the most typical result for this model structure. While these ensemble members explore the interactions between these land processes and climate feedback uncertainties, running a sufficiently large ensemble to determine the impact of each individual parameter has proved too computationally expensive to date. However there is a suggestion that two land surface parameters, *minLAI* and T_{OPT}, are related to the potential for large forest loss (Fig. 6),which due to their values in the standard configuration could partially explain the dieback observed in the standard model (Cox *et al.*, 2000), although we note that other parameters and climate changes are also important.

Perturbing parameters describing the physics and vegetation processes of the model generally leads to forests that are more resilient to future climate change over the next century than in the standard version. However large changes can still occur, especially under strong emissions scenarios where more loss or dieback is observed. In certain cases, slower increases in temperature and dry-season length under large CO_2 increases could lead to forest

454 growth (Fig, 7f, green shading). However in one member, a combination of perturbed
455 parameters cause forest resiliency that is low enough for differences in emissions scenarios to
456 be irrelevant for forest loss that shows considerable commitment to forest loss even by 2040.
457 The spread in results we find compared to the standard configuration highlights the
458 importance of fully exploring both parameter and future emission scenario uncertainty, as
459 well as trying to reduce it.

460 In our framework, dieback is caused by increased temperatures and dry-season lengths
461 caused by the increased atmospheric CO_2 which overwhelm the CO_2 fertilisation effect.
462 Visually, the movement of the individual grid points in the Amazon region towards the
463 boundary between conditions promoting sustainable forest and that unsuitable for forest is
464 faster than the movement of the boundary line itself (Fig. 3) in these cases. The increases in
465 CO_2 compared to the consequent increases in temperature and dry-season length could be
466 considered as a balance of expansion and risk of collapse and is important to consider when
467 planning mitigation strategy.

468 When decomposing the uncertainty in our framework, the climate change component appears
469 to be more important than forest resiliency. However both contribute to the total uncertainty.
470 This is more evident when we use observations as starting climate (comparing Fig. 9a to 9b),
471 which reduces uncertainty on where each grid point begins in our framework. It is worth
472 noting that we are assuming that the differences in 1950-1980 and 1860-1950 climates are
473 small relative to future changes, and that the forest stability has not markedly changed as a
474 result. A caveat here, is that we use the CO_2 fertilisation coefficient γ quantified from the
475 standard HadCM3LC model by Good *et al.*, (2011). We are, therefore, only exploring the
476 non-CO_2 fertilisation component of forest resiliency, and subsequently expect this framework

to underestimate the importance of the total forest resilience uncertainty, where the impact on CO_2 fertilisation (via changes to parameter γ) would also be accounted for.

DSR framework and validity of results

Our modified use of Good *et al.*'s DSR framework allows us to make predictions of committed change of the forest based on the emissions scenarios up to 2100. We note here that these predictions of committed change are 'lower bounds', meaning that more loss is likely to occur than we predict. Our assumption of the regression model we fit being linear breaks down at higher temperatures since this becomes a limiting factor in forest sustainability when we run a subset of the ensemble members to equilibrium (Fig. 4). The threshold for when this change in temperature sensitivity (α) begins to become significant is dependent on the optimum temperature (T_{OPT}) for photosynthesis in the model configuration (one of the major uncertainties in future tropical forest response (Booth *et al.*, 2012, Matthews *et al.*, 2007)). Nevertheless, the technique presented here represents a computationally efficient method of estimating the lower bound to simulated forest loss on the basis of the historical and future GCM climate and forest coverage. Future work could involve adding a non-linear temperature term into Eqn. (1) whilst exploring higher temperatures in true 2100 equilibrium runs.

The DSR framework provides a simple metric that can quantify why different models show markedly different responses. Given the uncertainty in current DVGM estimates, the DSR framework gives insight into moisture and temperature constraints and thus could be applied to other models, providing a simple comparison of some of the processes between them. Furthermore, the DSR framework could allow the relative contributions of temperature and DSL changes to forest loss to be calculated.

501 The inertia of the forest response found by Jones *et al.*, (2009) in the standard HadCM3LC
502 configuration may not be realistic. Whilst the response time of the forest to natural drought in
503 the real world (such as in 2005) appears to be within months (Phillips *et al.*, 2009), longer
504 term responses to less extreme but more sustained decreases in precipitation or increases in
505 temperature are yet to be determined. Drought experiments (Costa *et al.*, 2010) have shown a
506 slower decrease in tree mortality. This highlights the importance of improving DVGMs such
507 that they are able to create the short term responses to extreme drought, as well as the longer
508 term responses to slow increases in temperature and water stress, allowing us to reduce our
509 uncertainty in both the forest's transient and committed responses.

510

511 Implications of results

512 Our analysis compliments the work of Sitch *et al.*, (2008), Huntingford *et al.*, (2013) and
513 Poulter *et al.*, (2010). Sitch *et al.* (2008) explore uncertainties associated with a number of
514 DGVMs, when used with different emissions scenarios, whereas Huntingford *et al.* (2013)
515 explore the uncertainty associated with components of the climate response from a multi-
516 model ensemble which are then used to drive a common DGVM (based on
517 MOSES/TRIFFID). Huntingford *et al.*, (2013) also compare their results with the spread of
518 responses arising from parameter uncertainty in the land surface within a fully coupled GCM
519 (HadCM3C) that sampled uncertainties only in the vegetation component (Booth *et al.*,
520 2012). While Huntingford *et al.*, (2013)'s work suggests the forest will respond responsibly
521 well over the 21st century due to the CO_2 fertilization effect, Brienen *et al.*, (2015) suggest
522 that models showing more forest loss are more plausible. This suggests that there are still
523 open questions about the Amazon resilience to future climate changes.

524 Here we present results from new simulations (Booth *et al.*, 2013) that explore uncertainties
525 in both the land surface/vegetation response and the physical climate simultaneously. This
526 provides the first GCM ensemble where uncertainties in both physical climate and land
527 processes interact within a common experimental framework. Furthermore our approach to
528 determining uncertainty is very different from both of the previous works using our novel
529 dry-season resilience method. This allows us also to begin to determine where the
530 uncertainties lie. Poulter *et al.*, (2010) perturb parameters within the LPJmL DVGM more
531 extensively, and combine this with 8 different GCMs. Here we provide some uncertainty
532 associated with the TRIFFID DVGM, within a fully coupled framework where forest changes
533 both locally and globally feedback on the climate response, further exploring uncertainty.

534 In conclusion, we have highlighted the uncertainty in the Amazon rainforest's future due to
535 uncertainties in climate change and land based processes (in an experiment that explores a
536 broad range of vegetation and climate responses) and thus the importance of reducing these to
537 better determine the forest's outcome. Our predictions of committed rainforest change show
538 that even under the most intense mitigation, the forest may not be sustainable, despite
539 appearing to be at the end of the 21st century, suggesting that planning beyond 2100 is
540 essential.

541

542 **Acknowledgements**

543 We would like to thank Dr. Hugo Lambert for running the ocean spin-up model runs and Dr.
544 Doug McNeall for running the RCP 2.6 scenario for this ensemble. We use GPCC
545 precipitation data provided by the NOAA/OAR/ESRL PSD Boulder, Colorado, USA. Chris
546 Boulton was supported by a PhD studentship provided by the University of Exeter. The

547 contributions to this work from Ben Booth and Peter Good were supported by the Joint UK
548 DECC/Defra Met Office Hadley Centre Climate Programme (GA01101).

549

550 **References**

551 Booth BBB, Bernie D, Mcneall D *et al.* (2013) Scenario and modelling uncertainty in global mean
552 temperature change derived from emission-driven global climate models. *Earth Syst.*
553 *Dynam.,* **4**, 95-108.
554 Booth BBB, Jones CD, Collins M *et al.* (2012) High sensitivity of future global warming to land carbon
555 cycle processes. *Environmental Research Letters,* **7**, 024002.
556 Boulton C, Good P, Lenton T (2013) Early warning signals of simulated Amazon rainforest dieback.
557 *Theoretical Ecology,* **6**, 373-384.
558 Brienen RJW, Phillips OL, Feldpausch TR *et al.* (2015) Long-term decline of the Amazon carbon sink.
559 *Nature,* **519**, 344-348.
560 Brohan P, Kennedy JJ, Harris I, Tett SFB, Jones PD (2006) Uncertainty estimates in regional and global
561 observed temperature changes: A new data set from 1850. *Journal of Geophysical Research:*
562 *Atmospheres,* **111**, D12106.
563 Collins M, Booth BB, Bhaskaran B, Harris G, Murphy J, Sexton DH, Webb M (2011) Climate model
564 errors, feedbacks and forcings: a comparison of perturbed physics and multi-model
565 ensembles. *Climate Dynamics,* **36**, 1737-1766.
566 Collins M, Brierley CM, Macvean M, Booth BBB, Harris GR (2007) The Sensitivity of the Rate of
567 Transient Climate Change to Ocean Physics Perturbations. *Journal of Climate,* **20**, 2315-2320.
568 Costa ACLD, Galbraith D, Almeida S *et al.* (2010) Effect of 7 yr of experimental drought on vegetation
569 dynamics and biomass storage of an eastern Amazonian rainforest. *New Phytologist,* **187**,
570 579-591.

Cox PM (2001) Description of the 'TRIFFID' Dynamical Global Vegetation Model. *Hadley Centre Technical Note,* **24**.

Cox PM, Betts RA, Collins M, Harris PP, Huntingford C, Jones CD (2004) Amazonian forest dieback under climate-carbon cycle projections for the 21st century. *Theoretical and Applied Climatology,* **78**, 137-156.

Cox PM, Betts RA, Jones CD, Spall SA, Totterdell IJ (2000) Acceleration of global warming due to carbon-cycle feedbacks in a coupled climate model. *Nature,* **408**, 184-187.

Cox PM, Harris PP, Huntingford C *et al.* (2008) Increasing risk of Amazonian drought due to decreasing aerosol pollution. *Nature,* **453**, 212-215.

Cramer W, Bondeau A, Schaphoff S, Lucht W, Smith B, Sitch S (2004) Tropical forests and the global carbon cycle: impacts of atmospheric carbon dioxide, climate change and rate of deforestation. *Philosophical Transactions of the Royal Society of London. Series B: Biological Sciences,* **359**, 331-343.

Dirzo R, Raven PH (2003) Global state of bioversity and loss. *Annual Review of Environment and Resources,* **28**, 137-167.

Galbraith D, Levy PE, Sitch S, Huntingford C, Cox P, Williams M, Meir P (2010) Multiple mechanisms of Amazonian forest biomass losses in three dynamic global vegetation models under climate change. *New Phytologist,* **187**, 647-665.

Good P, Jones C, Lowe J, Betts R, Booth B, Huntingford C (2011) Quantifying Environmental Drivers of Future Tropical Forest Extent. *Journal of Climate,* **24**, 1337-1349.

Good P, Jones C, Lowe J, Betts R, Gedney N (2013) Comparing Tropical Forest Projections from Two Generations of Hadley Centre Earth System Models, HadGEM2-ES and HadCM3LC. *Journal of Climate,* **26**, 495-511.

Good P, Lowe JA, Collins M, Moufouma-Okia W (2008) An objective tropical Atlantic sea surface temperature gradient index for studies of south Amazon dry-season climate variability and

596 change. *Philosophical Transactions of the Royal Society B: Biological Sciences,* **363**, 1761-
597 1766.
598 Harris PP, Huntingford C, Cox PM (2008) Amazon Basin climate under global warming: the role of the
599 sea surface temperature. *Philosophical Transactions of the Royal Society B: Biological*
600 *Sciences,* **363**, 1753-1759.
601 Hirota M, Holmgren M, Van Nes EH, Scheffer M (2011) Global Resilience of Tropical Forest and
602 Savanna to Critical Transitions. *Science,* **334**, 232-235.
603 Huntingford C, Zelazowski P, Galbraith D *et al.* (2013) Simulated resilience of tropical rainforests to
604 CO2-induced climate change. *Nature Geosci,* **6**, 268-273.
605 Jones C, Lowe J, Liddicoat S, Betts R (2009) Committed terrestrial ecosystem changes due to climate
606 change. *Nature Geosci,* **2**, 484-487.
607 Lambert FH, Harris G, Collins M, Murphy J, Sexton DH, Booth BB (2013) Interactions between
608 perturbations to different Earth system components simulated by a fully-coupled climate
609 model. *Climate Dynamics,* **41**, 3055-3072.
610 Lenton TM (2011) Early warning of climate tipping points. *Nature Clim. Change,* **1**, 201-209.
611 Lenton TM, Held H, Kriegler E, Hall JW, Lucht W, Rahmstorf S, Schellnhuber HJ (2008) Tipping
612 elements in the Earth's climate system. *Proceedings of the National Academy of Sciences,*
613 **105**, 1786-1793.
614 Livina VN, Kwasniok F, Lenton TM (2010) Potential analysis reveals changing number of climate
615 states during the last 60 kyr. *Clim. Past,* **6**, 77-82.
616 Malhi Y, Aragão LEOC, Galbraith D *et al.* (2009) Exploring the likelihood and mechanism of a climate-
617 change-induced dieback of the Amazon rainforest. *Proceedings of the National Academy of*
618 *Sciences,* **106**, 20610–20615.
619 Malhi Y, Roberts JT, Betts RA, Killeen TJ, Li W, Nobre CA (2008) Climate Change, Deforestation, and
620 the Fate of the Amazon. *Science,* **319**, 169-172.

621 Matthews HD, Eby M, Ewen T, Friedlingstein P, Hawkins BJ (2007) What determines the magnitude
622 of carbon cycle-climate feedbacks? *Global Biogeochemical Cycles,* **21**, GB2012.
623 Meinshausen M, Raper SCB, Wigley TML (2008) Emulating IPCC AR4 atmosphere-ocean and carbon
624 cycle models for projecting global-mean, hemispheric and land/ocean temperatures:
625 MAGICC 6.0. *Atmospheric Chemistry and Physics Discussions,* **8**, 6153-6272.
626 Nakicenovic N, Alcamo J, Davis G, Other, Other, Other, Other (2000) *IPCC Special Report on Emission*
627 *Scenarios*, Cambridge.
628 Phillips OL, Aragão LEOC, Lewis SL *et al.* (2009) Drought Sensitivity of the Amazon Rainforest.
629 *Science,* **323**, 1344-1347.
630 Poulter B, Hattermann F, Hawkins ED *et al.* (2010) Robust dynamics of Amazon dieback to climate
631 change with perturbed ecosystem model parameters. *Global Change Biology,* **16**, 2476-
632 2495.
633 Rammig A, Jupp T, Thonicke K *et al.* (2010) Estimating the risk of Amazonian forest dieback. *New*
634 *Phytologist,* **187**, 694-706.
635 Riahi K, Grübler A, Nakicenovic N (2007) Scenarios of long-term socio-economic and environmental
636 development under climate stabilization. *Technological Forecasting and Social Change,* **74**,
637 887-935.
638 Salazar LF, Nobre CA, Oyama MD (2007) Climate change consequences on the biome distribution in
639 tropical South America. *Geophysical Research Letters,* **34**, n/a-n/a.
640 Schneider U, Becker A, Finger P, Meyer-Christoffer A, Ziese M, Rudolf B (2014) GPCC's new land
641 surface precipitation climatology based on quality-controlled in situ data and its role in
642 quantifying the global water cycle. *Theoretical and Applied Climatology,* **115**, 15-40.
643 Scholze M, Knorr W, Arnell NW, Prentice IC (2006) A climate-change risk analysis for world
644 ecosystems. *Proceedings of the National Academy of Sciences,* **103**, 13116-13120.
645 Shiogama H, Emori S, Hanasaki N, Abe M, Masutomi Y, Takahashi K, Nozawa T (2011) Observational
646 constraints indicate risk of drying in the Amazon basin. *Nat Commun,* **2**, 253.

Sitch S, Huntingford C, Gedney N *et al.* (2008) Evaluation of the terrestrial carbon cycle, future plant geography and climate-carbon cycle feedbacks using five Dynamic Global Vegetation Models (DGVMs). *Global Change Biology,* **14**, 2015-2039.

Spracklen DV, Arnold SR, Taylor CM (2012) Observations of increased tropical rainfall preceded by air passage over forests. *Nature,* **489**, 282-285.

Van Vuuren DP, Eickhout B, Lucas PL, Den Elzen MGJ (2006) Long-Term Multi-Gas Scenarios to Stabilise Radiative Forcing - Exploring Costs and Benefits Within an Integrated Assessment Framework. *The Energy Journal,* **27**, 201-233.

Van Vuuren DP, Elzen MJ, Lucas P *et al.* (2007) Stabilizing greenhouse gas concentrations at low levels: an assessment of reduction strategies and costs. *Climatic Change,* **81**, 119-159.

White A, Cannell MGR, Friend AD (1999) Climate change impacts on ecosystems and the terrestrial carbon sink: a new assessment. *Global Environmental Change,* **9, Supplement 1**, S21-S30.

660 **Table**

Parameter	Range (for broadleaf FPT)	Description
f0	0.72-0.95	Maximum ratio of internal to external CO2 concentration – related to stomatal resistance
minLAI	1-4	Minimum Leaf Area Index (green leaf area per unit ground) needed before a PFT competes for space
N_{LO}	0.018-0.1 kgN/kgC	Top leaf nitrogen concentration
Q10	1.5-3.5	Temperature dependence on soil respiration
T_{OPT}	27-37 (°C)	Optimum temperature for photosynthesis
Θ_{CRIT}	0.01-0.99	Critical value of volumetric soil moisture, below which soil moistures limits plant photosynthesis and surface evaporation

661 Table 1: Ranges and descriptions of perturbed parameters in the carbon cycle component of

662 HadCM3C-ESE, as detailed by Booth *et al.*, (2012)

663 **Figures**

664

665 **Figure 1** A comparison of the starting temperatures and dry-season lengths (DSLs) for members of
666 HadCM3C-ESE and the observed climate using the mean Amazon rainforest states. a) The position of
667 the starting state for the average Amazon rainforest for each ensemble member (black circles) shown
668 alongside the observed average Amazon rainforest state (red square). Cumulative probability
669 distributions (the proportion of models showing at least the value on the x-axis) are shown for both (b)
670 temperature and (c) DSL for the ensembles with the observed climate shown by dotted lines in each
671 case.

672

673

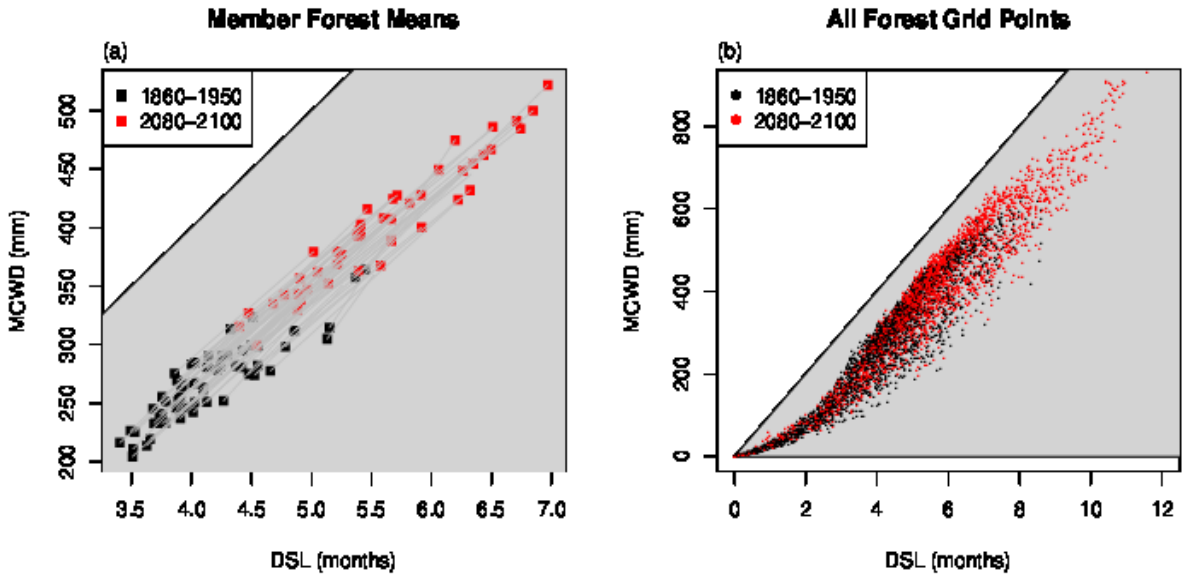

674

675 **Figure 2** A comparison of dry-season length (DSL) and maximum cumulative water deficit (MCWD)
676 in the HadCM3C-ESE under the A1B scenario. (a) Ensemble member forest region means and (b) all
677 forest grid point across all ensemble members' DSL values are plotted against their MCWD values for
678 the 1860-1950 mean state (black) and the 2080-2100 mean state (red). In (a), ensemble members'
679 states are connected by a dark grey line. The light grey background shows the envelope of possible
680 values for DSL and MCWD.

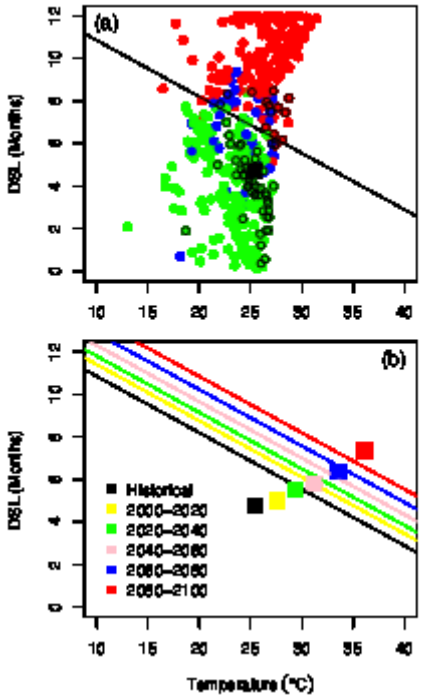

681

682 **Figure 3** Estimating dry-season resilience (DSR) for a typical ensemble member. (a) The
683 historical (1860-1950) mean temperature and dry-season length (DSL) is observed for all
684 tropical grid boxes (20°S -20°N) which are then plotted in the temperature-DSL plane. The
685 colour of each grid boxes' point is green for 'Forest' ($BL > 0.4$), blue for 'Intermediate' (0.4
686 $< BL < 0.05$) or red for 'No Forest' ($BL < 0.05$). The DSR=0 line (as described in main text)
687 is shown by a black line. Circled points are those contained with the region 40°-70°W, 15°S-
688 5°N (the Amazon region) and the black square is the mean state of the Amazon forest (green
689 circled points). (b) Future changes in atmospheric CO2, temperature and DSL move both the
690 DSR=0 line and the position of the points (represented here by the mean Amazon forest state,
691 black square) which are tracked in 20 year averages over the 21st century.

692

693 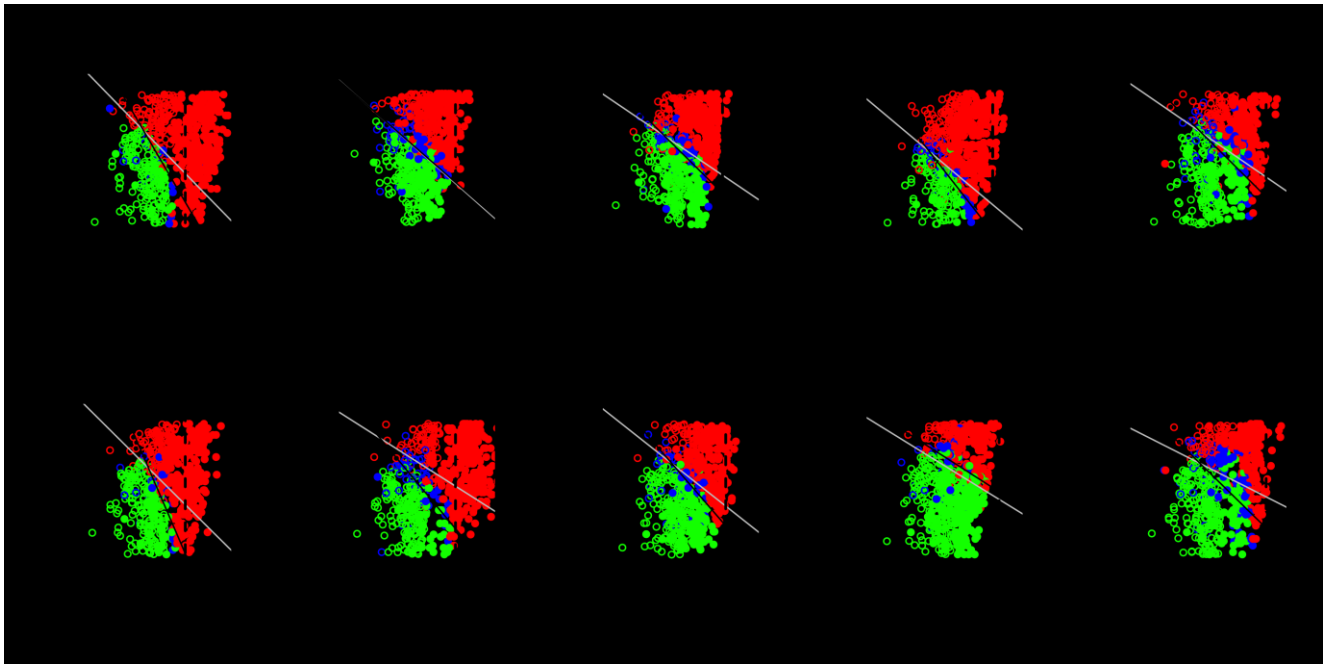

694 **Figure 4** The effect of the parameter T_{OPT} on the DSR=0 line for the 10 equilibrium runs. Plots are
695 ordered in increasing value of T_{OPT}. Hollow points are data from the transient historical (1860-1950)
696 and filled points are from the equilibrium run. The DSR=0 line is shown when fitted only with the
697 transient data (grey) and with all the data (black).

698

699

700

701

702

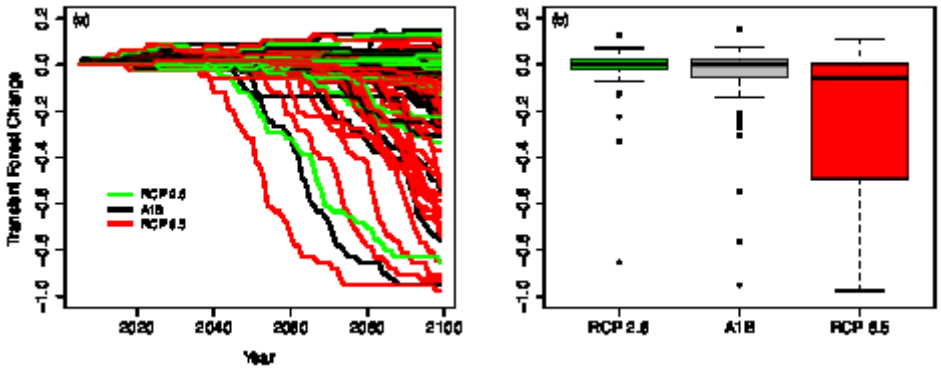

703

704 **Figure 5** Transient changes in number of grid boxes containing Amazon forest (BL fraction
705 > 0.4 within the region 40°-70°W, 15°S-5°N) in HadCM3C-ESE compared to historical
706 (1860-1950) Amazon forest coverage. (a) Time series of this transient changes for each
707 individual member of HadCM3C-ESE. (b) Box and whisker plots for each scenario showing
708 the median, inter-quartile range and minimum and maximum values (ignoring outliers, black
709 circles).

710

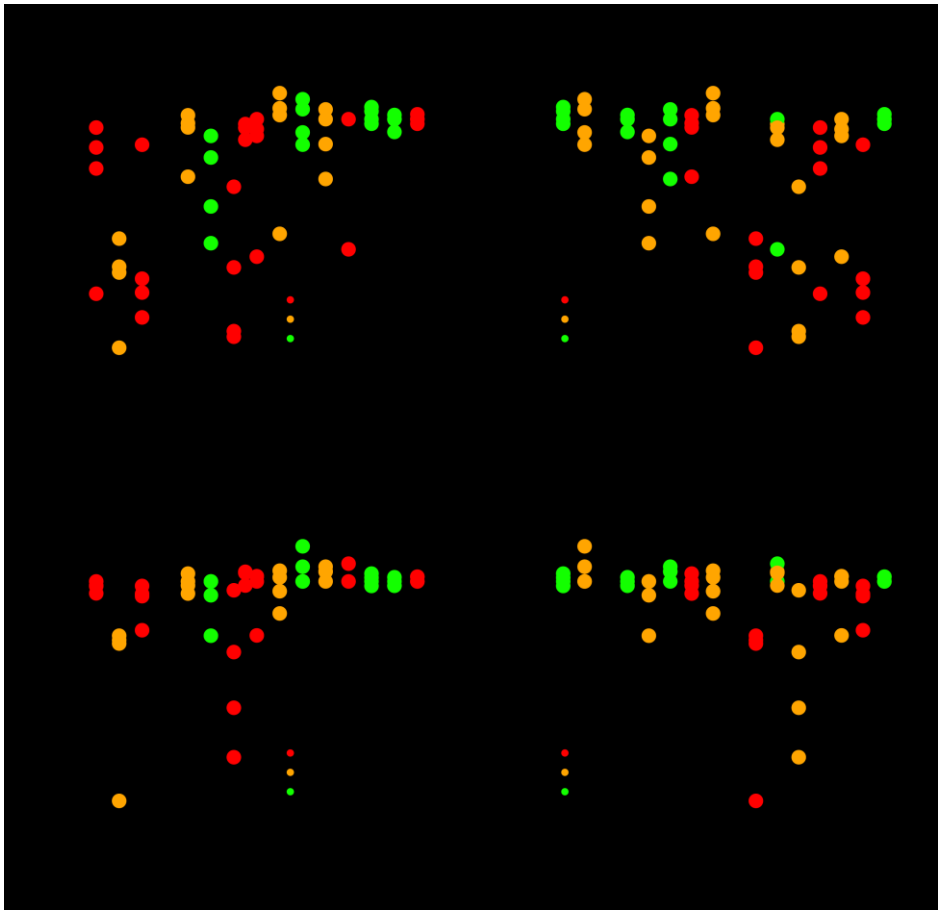

711

712 **Figure 6** The effect of perturbing parameters on transient forest change by 2100. Proportional forest
713 change observed in ensemble members under scenarios (a,b) RCP 8.5 and (c,d) A1B scenarios are
714 plotted against the (a,c) T_{OPT} and (b,d) *minLAI* values of each member. The colours of points show the
715 value of the parameter not plotted.

716

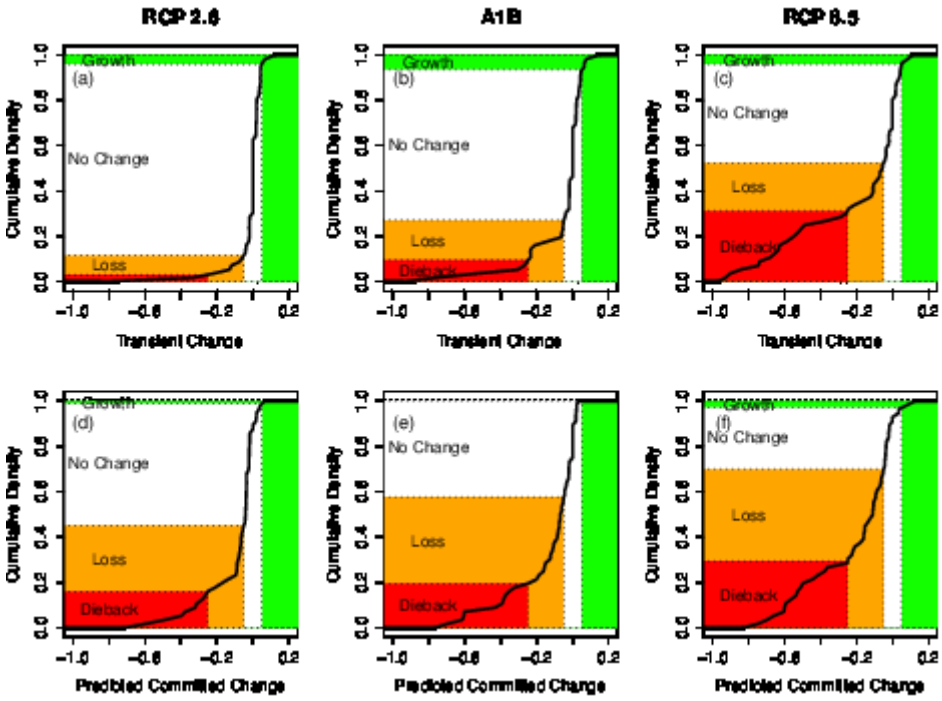

717

718 **Figure 7** Summary CDFs of the Amazon rainforest fractional changes in grid boxes deemed
719 forest for ensemble members of HadCM3C-ESE. Transient responses observed by 2100 for
720 scenarios (a) RCP 2.6, (b) A1B and (c) RCP 8.5 are shown above predicted committed
721 responses using the DSR method for (d) RCP 2.6, (e) A1B and (f) RCP 8.5. Coloured regions
722 show proportion of models which show changes we class as 'Dieback' (red, < -25%), 'Loss'
723 (orange, >-25%,<-5%), 'No Change' (white, >-5%, <5%) and 'Growth' (green, >5%).

724

725

726

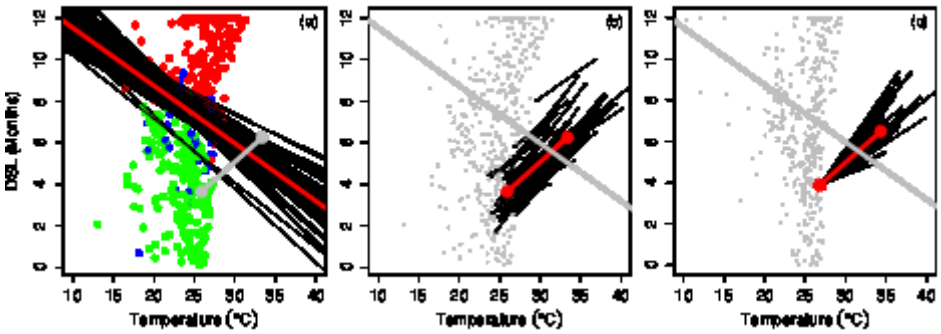

727

728 **Figure 8** Graphical representations of how (a) forest resiliency, (b) climate and (c) climate
729 (including observations) are constrained. In all cases black lines represent values from
730 individual ensemble members, red lines represent the values used when the variable is
731 constrained and grey lines represent how the other variable is constrained. Points shown in
732 the background are from (a,b) a typical ensemble member or (c) observations. The same point
733 (in the Amazon region) is used when demonstrating constraining climate and climate
734 (including observations).

735

736

737

738

Figure 9 CDFs showing predicted committed Amazon forest change for the RCP 8.5 scenario. Committed change is predicted using (a) the 1860-1950 modelled state (temperature and dry-season lengths; as in Fig. 7f) and (b) real world observations (see main text). Committed change is also predicted whilst keeping resilience parameters constant (dashed lines) and climate change constant (dotted lines). Constraining one variable allows the uncertainty in the other to be explored (as described in text).